Relationships Between Thermally Induced Residual Stresses and Architecture of Epoxy-Amine Model Networks

DIDIER BAUCHIERE,[1]* JEAN LOUIS HALARY,[1] LUCIEN MONNERIE,[1] ROBERT SCHIRRER[2]

[1] Laboratoire de Physicochimie Structurale et Macromoléculaire (UMR 7615), Ecole Supérieure de Physique et de Chimie Industrielles de la Ville de Paris, 10, rue Vauquelin, 75231 Paris Cedex 05, France

[2] Institut Charles Sadron, 6, rue Boussingault, 67083 Strasbourg Cedex, France

Received 11 March 1999; accepted 31 May 1999

ABSTRACT: The capability of epoxy-amine resins to develop residual stresses was studied as a function of temperature and network architecture. These residual stresses were induced while cooling epoxy-glass bilayers from temperatures higher than the network glass transition temperature, T_g. This behavior was the result of the marked differences $(\alpha_{r'} - \alpha_g)$, in linear thermal expansion coefficient of the two components, as evidenced by the measurement of $\alpha_{r'}$ for the epoxy networks under study. Various network architectures were selected, resulting from variation of (1) the chemical nature of both epoxide and curing agent, (2) the nature and relative amount of the chain-extensor agent, and (3) the stoichiometric ratio. Three ranges of cooling temperature were observed systematically: first, the range of temperatures above T_g, where no stress has been detected, then an intermediate temperature range (from T_g to T^*), where stresses develop quite slowly, and finally, the low temperature range ($T < T^*$), where a linear increase in stress accompanies the decrease of temperature. The two latter regimes were quantitatively characterized by the extent, $T_g - T^*$, of the first one and by the slope, SDR, of the second one. $T_g - T^*$ values were shown to be governed by the T_g of the network: the higher the T_g, the larger the gap between T_g and T^*. This result was interpreted by accounting for the variation of relaxation rate at T_g from one network to the other. It was also shown that a semiempirical relationship holds between SDR and T_g: SDR decreases monotonically as T_g increases. By inspecting the effects of network architecture in more details, it turned out that SDR is governed by the Young's moduli, $E_{r'}(T - T_g)$, of the epoxy resins in the glassy state: the lower $E_{r'}(T - T_g)$, the lower SDR in a series of homologous networks. As $E_{r'}(T - T_g)$ values are known to be related to the characteristics of the secondary relaxation β, which depends, in turn, on crosslink density, SDR values were finally connected to the amplitude of the β relaxation processes. This finding was corroborated by the measurements on an antiplasticized dense network. Finally, data relative to thermoplastic-filled networks showed that the addition of thermoplastic reduces the development of residual stresses, whatever the system, is homogeneous or biphasic. © 2000 John Wiley & Sons, Inc. J Appl Polym Sci 75: 638–650, 2000

Key words: epoxy networks; residual stresses; thermal expansion coefficient; viscoelastic behavior; glass transition; secondary relaxation; thermoplastic-filled epoxies; antiplasticizer

INTRODUCTION

Epoxy resins are used in a wide range of industrial applications, as the result of their versatile properties. In particular, they are demanded as matrices for fiber-reinforced composites including

Correspondence to: J. L. Halary.
* *Present address:* CEBAL, Research Center, P.O. Box 16, 51801 Sainte-Ménehould, France.
Contract grant sponsor: DGA/DRET; contract grant number: 92 18.B/DRET.

Journal of Applied Polymer Science, Vol. 75, 638–650 (2000)
© 2000 John Wiley & Sons, Inc. CCC 0021-8995/00/050638-13

either glass fibers in regular materials or carbon fibers in high-performance composites.

Epoxy resins have been extensively studied for years, but, despite the number of reports and reviews available in the literature,[1–3] the understanding of the connection between the chemical structure and the mechanical properties of these materials remains limited, probably as the result of the complexity of the commercial formulations. The influence of network architecture on the properties of the matrices has been clarified by using series of model systems, designed to present a systematic variation of the network rigidity while keeping the crosslink density constant, and vice versa.[4–7] Thus, unambiguous results were obtained dealing with the glass transition temperature T_g,[5,7–9], the free volume,[10] the secondary relaxation β,[5,11,12] and the antiplasticization phenomenon.[13,14]

In the case of composites, additional pending questions refer to the interaction between matrix and fiber. It is known, for instance, that undesired thermally induced stresses develop at the end of the preparation of the glass–epoxy composite pieces while cooling the samples from cure temperatures above T_g down to room temperature.

Modeling of these stresses has already be done in the case of polyurethanes by Aboulfaraj et al.[15,16] Their approach is based on the preparation and observation of polyurethane–glass bilayers. In that case, the development of residual stresses upon cooling can be quantitatively followed either by measuring the progressive bending of free bilayers by laser interferometry or by measuring the external load, which has to be applied on the bilayer to keep it undeformed. It is the latter procedure that has been retained in the present study, because of its easiness to be adapted on commercial testing systems.[17]

From a physical viewpoint, the formation of thermally induced stresses in the bilayers is the result of the balance between two opposed effects. There is, on the one hand, a driving force for producing residual stresses upon cooling, which is the difference of thermal expansion coefficients of the resin and of glass, and, on the other hand, a temperature-dependent capacity of the networks to relax the induced stresses. It has been shown,[15,16] from simple mechanical calculations, that one can account well for the observed phenomena by using the equation

$$\sigma_r = \frac{E_r E_g b \Delta T(\alpha_g - \alpha_r)}{E_r a + E_g b} \tag{1}$$

where the subscripts r and g refer to the resin and glass, respectively, E and α are the Young's modulus and linear thermal expansion coefficient, respectively, and a and b are the thicknesses of the epoxy resin and glass layers, respectively.

Because changes in network architecture are supposed to be accompanied by changes in both E_r and α_r, one may expect that they affect, in turn, the extent of residual stresses.

The goal of the present work is to provide an understanding of the connections between the capacity of the networks to develop residual stresses and (1) their rigidity (which is a function of their chemical structure), and (2) their crosslink density (which can depend on formulation, stoichiometric ratio, and extent of reaction). To achieve this goal, model epoxy networks were considered once more, in the form of epoxy–glass bilayers. Additional survey of the properties of antiplasticized and thermoplastic-filled samples was used as a mean to examine the situation in the presence of more complex formulations.

EXPERIMENTAL

Materials

Chemicals

Diglycidylether of bisphenol A (DGEBA) and diglycidylether of resorcinol (DGERO) were purchased from Bakelite Co. (grade Rutapox 0162) and Lancaster, respectively. They were used as received, owing to their high purity and very low degree of polymerization. Diglycidylether of 1,4-butanediol (DGEBU) was purchased from Acros Organics and was fractionated by distillation under reduced pressure before use. The fraction considered in this study had a boiling point of 70°C under 0.06 Torr.

Diaminodiphenylmethane (DDM) was purchased from Acros Organics, whereas hexamethylenediamine (HMDA), hexylamine (HA) and *NN′*-hexamethylenediamine (DMHMDA) were purchased from Aldrich. All these high-purity chemicals were used as received. The noncommercial chemicals 4-benzylaniline (BAN) and *N,N′*-dimethyldiaminodiphenylmethane (DMDDM), of chemical formulae

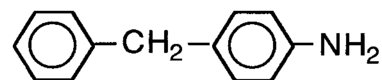

and

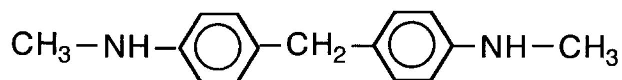

respectively, have been synthesized and purified in our laboratory by Dr. B. Jasse and Mrs F. Costa-Torro according to well-documented methods.[18,19]

The antiplasticizer (AP) used in this study has for chemical formula

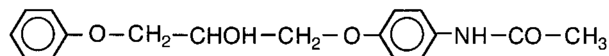

as the result of the reaction of epoxyphenoxypropane and hydroxyacetanilide. AP was synthesized in our laboratory by following a procedure detailed elsewhere;[13,20] it was obtained in the form of a yellow amorphous material, and was used without further purification.

Polyethersulfone (PES), a thermoplastic polymer of high glass transition temperature (T_g = 230°C) whose chemical formula is

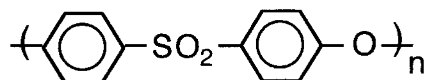

was purchased from Goodfellow Ltd. No information is available on molecular weight and polydispersity of the batch used.

Network Preparation Procedures

Diglycidylether of bisphenol A (DGEBA) was heated up at 50°C and briefly degassed under vacuum before the addition of amine(s). This step is ommitted in the case of diglycidylethers of resorcinol and 1,4-butanediol (DGERO and DGEBU), which are liquid at room temperature. Dissolution of the amines was performed under nitrogen gas, at 35°C in the case of aliphatic amines, and at 80°C in the case of aromatic ones. The typical cure cycle consisted of a 2-h step at temperatures below the exotherm, followed by a 12-h period at the exotherm, and finally a 24-h postcure at 30°C above T_g.

The same procedure was used for preparing the antiplasticized network, except that AP was added to the diepoxide and heated at 60°C under stirring, and that the degassing step was delayed until an homogeneous mixture is obtained. The amount of AP was fixed to 19 wt % of the starting formulation (diepoxide + hardener + AP).

In the case of the thermoplastic-modified networks, a 10 wt % solution of PES in dichloromethane was first prepared under stirring, and then the diepoxide was poured to the solution under continuous stirring until an homogeneous mixture is formed. Later on, most of the solvent was slowly evaporated by progressive heating up to 80°C. Complete removal of the solvent was achieved by further heat treatment at 100°C under vacuum for 12 h. Then, the hardener was added and the mixture was kept at 80°C under stirring until complete dissolution. Finally, two different cure procedures were used, both starting at 100°C. The first one is a progressive heating, consisting in the succession of six 2-h steps spaced from each other by an increase in temperature of 20°C, and followed by a postcure at 220°C for 24 h: the samples thus obtained, so called H, are transparent and are expected to be homogeneous. The alternative cure procedure is performed under nitrogen atmosphere; it consists in a heating step, as rapid as possible, from 100 to 240°C, followed by an isothermal step of 24 h at 240°C. The samples thus obtained, so called B, are opaque and typical of phase-separated materials.

The setup used for curing the samples depended on whether free epoxy sheets or glass-supported epoxy layers were prepared. In the former case, cure and postcure were performed, according to the thermal conditions mentioned above, in a stainless steel mold equipped with its own regulated heating system. Sheets of 100 × 100 × 3 mm^3 were obtained, from which the samples for viscoelastic measurements were cut to the desired size by using a laboratory saw Krautkramer Isomet. As far as the epoxy–glass bilayers are concerned, glass disks of thickness b = 2 mm and radius l = 50 mm were carefully cleaned with a sulfochromic mixture and then attached to a silicone seal, which allows deposition on the glass disk of a layer of monomer mixture to an approximative thickness of 1 mm. Cure and postcure were carried out in a oven under a controlled atmosphere. The actual thickness a of the epoxy layer was measured during the cure cycle, just after the gel point has been passed. At the end of the postcure, the bilayers were kept at 20°C above the glass transition temperature T_g until the residual stress measurements. Otherwise, they exhibit a progressive curvature along the cooling step and then break.

Network Designation and Crosslink Density

As shown in Table I, the samples are coded by accounting primarily for the nature of both diep-

Table I Designation and Formulation of the Networks Under Study

Network Code	Diepoxide	Primary Diamine Hardener	Difunctional Cohardener	Additive	Theoretical Crosslink Density (mol · L^{-1})
A-1-DDM	DGEBA (2 mol)	DDM (1 mol)	None	None	2.71
A-1-BAN60	DGEBA (5 mol)	DDM (1 mol)	BAN (3 mol)	None	0.97
A-1-BAN80	DGEBA (10 mol)	DDM (1 mol)	BAN (8 mol)	None	0.47
A-1-BAN95	DGEBA (40 mol)	DDM (1 mol)	BAN (38 mol)	None	0.11
A-1-DMDDM60	DGEBA (5 mol)	DDM (1 mol)	DMDDM (3 mol)	None	0.98
A-0.7-DDM	DGEBA (2.857 mol)	DDM (1 mol)	None	None	0.29
A-0.8-DDM	DGEBA (2.5 mol)	DDM (1 mol)	None	None	1.14
A-0.9-DDM	DGEBA (2.222 mol)	DDM (1 mol)	None	None	1.94
A-1.1-DDM	DGEBA (1.818 mol)	DDM (1 mol)	None	None	2.39
A-1.2-DDM	DGEBA (1.667 mol)	DDM (1 mol)	None	None	2.08
A-1.3-DDM	DGEBA (1.538 mol)	DDM (1 mol)	None	None	1.78
A-1-DDM/AP	DGEBA (2 mol)	DDM (1 mol)	None	AP (19 wt %)	2.71
A-1-DDM/PES-H	DGEBA (2 mol)	DDM (1 mol)	None	PES (11 wt %)	
A-1-DDM/PES-B	DGEBA (2 mol)	DDM (1 mol)	None	PES (11 wt %)	
A-1-HMDA	DGEBA (2 mol)	HMDA (1 mol)	None	None	2.92
A-1-HA60	DGEBA (5 mol)	HMDA (1 mol)	HA (3 mol)	None	1.08
A-1-DMHMDA60	DGEBA (5 mol)	HMDA (1 mol)	DMHMDA (3 mol)	None	1.00
O-1-DDM	DGERO (2 mol)	DDM (1 mol)	None	None	3.95
O-1-BAN60	DGERO (5 mol)	DDM (1 mol)	BAN (3 mol)	None	1.33
O-1-DMDDM60	DGERO (5 mol)	DDM (1 mol)	DMDDM (3 mol)	None	1.23
O-1-HMDA	DGERO (2 mol)	HMDA (1 mol)	None	None	4.42
O-1-HA60	DGERO (5 mol)	HMDA (1 mol)	HA (3 mol)	None	1.55
O-1-DMHMDA60	DGERO (5 mol)	HMDA (1 mol)	DMHMDA (3 mol)	None	1.42
U-1-DDM	DGEBU (2 mol)	DDM (1 mol)	None	None	3.95
U-1-BAN60	DGEBU (5 mol)	DDM (1 mol)	BAN (3 mol)	None	1.34
U-1-DMDDM60	DGEBU (5 mol)	DDM (1 mol)	DMDDM (3 mol)	None	1.23

oxide and hardener(s) and for the stoichiometric ratio r, which is the ratio of the number of N—H groups to the number of epoxide rings in the initial mixture: A, O, and U stand for DGEBA, DGERO, and DGEBU, respectively; r ranges from 0.7 to 1.3, with a value of 1 for the stoichiometric systems; the hardener is represented by the acronym of the primary diamine or of the difunctional cohardener in the case of binary and ternary mixtures, respectively. In the later case, the additional figure represents the mol percentage of the total NH functions that come from the cohardener. As an example, the code O-1-HA60 refers to the network made from stoichiometric proportions of diglycidylether of resorcinol, hexamethylenediamine, and hexylamine, with 60 mol % of the NH functions coming from the hexylamine molecules; based on 1 mol of HMDA, that corresponds to relative amounts of 5 mol of DGERO and 3 mol of HA. Eventually, the additional mention of /AP, /PES-H, and /PES-B indicates the presence of an additive in the initial mixture, namely the antiplasticizer AP and the polyethersulfone PES, respectively. In the later case, as mentioned above, H and B refer to the morphology of the network, either homogeneous (H) or biphasic (B).

The last entry of Table I gives the so-called theoretical crosslink density of the various networks. This quantity, whose determination is detailed in a previous publication,[7] would coincide with the true crosslink density, if the actual extents of reaction were unity.

Thermomechanical Measurements

All the experiments reported in this section were performed by using a servohydraulic testing system MTS 831, equipped with a well-regulated temperature chamber (temperature fluctuations less than 0.5°C in isothermal conditions).

Viscoelastic Measurements

A sample of 70 × 12 × 3 mm^3 was subjected in isothermal conditions to a static tensile strain of about 0.1%, on which a sinusoidal tensile strain of frequency 1 Hz and of amplitude as small as ±0.05% was superimposed. Analysis of the relevant complex stress yielded the tensile storage

modulus, E', and loss modulus E''. The temperature increment between two consecutive measurements was 2°C, and the overall temperature range under study extended from −90°C to T_g + 30°C. According to the observations made in previous articles,[8,21,22] the glass transition temperature T_g was supposed here to be identical to the temperature at which the E'' goes through a maximum when the frequency is 1 Hz.

Measurement of the Thermal Expansion Coefficient in the Glassy State

A sample of 50 × 10 × 2 mm^3 was attached to the fixtures of the testing machine at room temperature, and then the temperature chamber was cooled down to the lowest temperature under study, i.e. −80°C. After a thermal equilibration time of 1 h for both sample and fixtures, the system was placed under stress control at a level equal to zero stress, whereas the value of the displacement was also set to zero. Then a temperature increment of 20°C was applied, and the displacement at zero stress was measured after an equilibration time of 1 h, and so on, until the glass transition temperature is approached. Use of a proper calibration curve, accounting in particular for the expansion of the testing system fixtures inside the chamber, allowed extraction the value of the thermal expansion coefficient, α_r, of the polymeric network in the glassy state from the displacement values. The suitability of this procedure was checked in the case of standards including aluminum and polystyrene for which accurate values of α are available in the literature:[23] it turned out that the uncertainty on our measurements may be estimated to $\pm 3 \cdot 10^{-6}$ K^{-1}.

Measurement of the Thermally Induced Stresses in the Epoxy–Glass Bilayers

The experimental procedure described in this section is just the adaptation on a commercial testing system of that used by Aboulfaraj and Schirrer in an earlier work.[15,16] The reader should return to the original publications to get information on the theoretical bases of the method, which fall out of the scope of the present article. Two strong assumptions are made in the calculations: (1) absence of residual stresses at and above T_g + 20°C, and (2) perfect adhesion between the glass layer and the polymeric layer. The validity of the former assumption is discussed below, in the Results section. Regarding the latter, the adhesion between the two layers is probably excellent in our systems, as the result of strong interactions existing between the silanol groups present at the surface of the glass layer and the OH functions of the hydroxypropylether groups, which are formed in the networks by opening of the epoxide rings along the step-polymerization process (see, e.g., ref. 4).

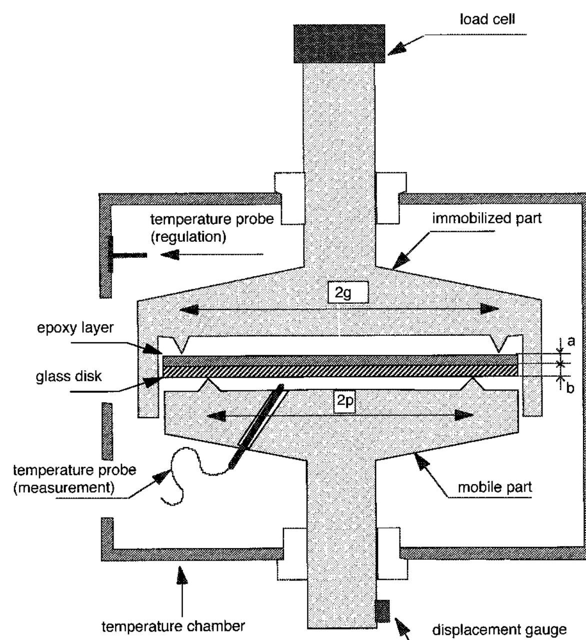

Figure 1 Schematic presentation of the setup designed for measuring the residual stresses (typical dimensions: a = 1 mm; b = 2 mm; p = 37.5 mm; g = 45 mm).

Setup[17]

Experiments were performed by using a servohydraulic testing system MTS 810, equipped with a temperature chamber covering the range from −120 to 250°C, with an accuracy better than 1°C, and with a high-sensitivity load cell (full scale of 500 N, resolution equal to 0.1% of the full scale) and displacement gauge (resolution equal to 1 μm). A routine MTS "Testlink 2" was used: (1) to monitor the cooling down of the temperature chamber at a rate of 2 K · min^{-1} or 4 K · min^{-1}; (2) to record in real time the strength, F, detected by the load cell and the actual temperature of the sample; and (3) to reset the displacement to zero every 5°C as an account for the contraction upon cooling of the testing system fixtures inside the chamber (on average, this displacement correction was around 10 μm per 1°C). As shown in Figure 1, a special sample holder, of cylindrical

symmetry, replaced the usual grips of the MTS 810 machine.

Measurement Procedure

An epoxy–glass disk, prepared as described above and then kept in a vacuum oven at the temperature (T_g + 20°C), was rapidly transferred inside the testing system chamber, preheated at the same temperature, and put on the top of the mobile part of the sample holder (Fig. 1). Then the hydraulic actuator of the machine was run until the sample come in close contact to the immobilized part, the criterium for this achievement being the detection by the load cell of a strength of 2 *N*. At that time, the displacement of the mobile part was set to zero, and the "Testlink 2" routine was activated in order to record, as a function of time, the changes in the sample actual temperature and strength, F, required to maintain the bilayer undeformed while it is cooled down at constant rate.

Experimental Data Processing

The thermally induced residual stresses, σ_r, were derived from the strength values, F, thanks to the equation[15,16]

$$\sigma_r = \frac{2}{a(a+b)}\left[\frac{(1-\nu)(g^2-p^2)}{8\pi g^2} - \frac{(1+\nu)\ln(p/g)}{4\pi}\right]F \quad (2)$$

where a, b, g, and p are experimental dimensions (see Fig. 1) and ν is the Poisson ratio.

The values of σ_r were calculated by the computer every 5°C along the cooling step, starting at T_g + 20°C.

RESULTS AND DISCUSSION

Thermal Characteristics of the Networks

Most of the values of glass transition temperature, T_g, given in the first entry of Table II have already been published and discussed elsewhere.[5,7] As a general rule, these values are in satisfactory agreement with earlier reports; sometimes they are higher, because of our severe postcure procedure, which permits optimization of the extent of reaction.[28] The fact that the T_gs of the additive-free materials range from 28 to 188°C is a further illustration of the huge influences of chain rigidity, crosslink density, and presence of dangling moities. In the presence of the additive AP, the depression of T_g towards the pure network has been interpreted as a plasticization of the chains in this temperature range.[25] Finally, the T_gs observed in the presence of thermoplastic additive are just what one should expect: a unique T_g is detected in the homogeneous blend, whereas two T_gs (close to those of the pure components) are observed in the biphasic system.

The second entry of Table II gives our measurements of the linear thermal expansion coefficients, α_r, of the resins in the glassy state. With the exception of the network A-1-HMDA, the range of measured values is quite narrow (from $55 \cdot 10^{-6}$ K^{-1} to $64 \cdot 10^{-6}$ K^{-1}), and in satisfactory agreement with previous determinations.[10,27] Considering the accuracy on the measurements ($\pm 3 \cdot 10^{-6}$ K^{-1}), this prevents any suitable statement on the possible connection of α_r with crosslink density and presence of dangling moities. The quite peculiar value observed for the network A-1-HMDA ($83 \cdot 10^{-6}$ K^{-1}) seems to be acceptable, in the sense that it corresponds to the mean value of two independent results of the literature.[10,27] Our result perhaps emphasizes the influence of the flexibility of the —$(CH_2)_6$— moities on the value of the thermal expansion coefficient. To some extent, the fact that the values of α_r found for A-1-HA60, A-1-DMHMDA60, and O-1-HMDA are unambiguously higher than that of their aromatic counterpart A-1-BAN60, A-1-DMDDM60, and O-1-DDM, respectively (Table II) might corroborate this tentative conclusion.

General Shape of the Plots of Residual Stress vs. Temperature

Figure 2 shows an example of plot of σ_r vs. temperature. It is relative to the network A-1-HA60, but all the systems behave qualitatively in the same manner. The plots can be conventionally divided in three temperature ranges: (1) the high-temperature range (range A), over which σ_r remains equal to zero within the sensitivity of the measurements; 2) the low-temperature range (range B), where σ_r increases linearly with decreasing temperature; and (3) an intermediate temperature range (range C), marked by a smooth linking up of the ranges A and B. As can also be seen in Figure 2, which has been drawn by using the data relative to two separate experiments, the reproducibility of the measurements is excellent. This allows one to argue quantitatively

Table II Thermal Characteristics of the Networks

Network	Glass Transition Temperature T_g (°C)	Thermal Expansion Coefficient $10^6 \times \alpha_r$ (K^{-1})
A-1-DDM	188[181[10], 184–185[24]]	64[64[10], 59[27]]
A-1-BAN60	115	58
A-1-BAN80	101	59
A-1-BAN95	86	62
A-1-DMDDM60	113	58
A-0.7-DDM	96	62
A-0.8-DDM	144	55
A-0.9-DDM	182	61
A-1.1-DDM	177	62
A-1.2-DDM	164	61
A-1.3-DDM	153	56
A-1-DDM/AP	107[106[25]]	63
A-1-DDM/PES-H	183	62
A-1-DDM/PES-B	188/220	62
A-1-HMDA	121[119[10], 118[24]]	83[74[10], 91[27]]
A-1-HA60	70[68[10], 64[24]]	63[67[10]]
A-1-DMHMDA60	60[51[6]]	64
O-1-DDM	144[135[10], 123[26]]	58[58[10]]
O-1-BAN60	85	57
O-1-DMDDM60	81	58
O-1-HMDA	84[78[10], 79[26]]	63[55[10]]
O-1-HA60	44[42[10]]	61[64[10]]
O-1-DMHMDA60	30	60
U-1-DDM	78[76[6]]	64
U-1-BAN60	32	63
U-1-DMDDM60	28	60

The values in brackets are taken from the literature.

from even the slight differences observed, from one network to the other, on the plots of σ_r vs. temperature.

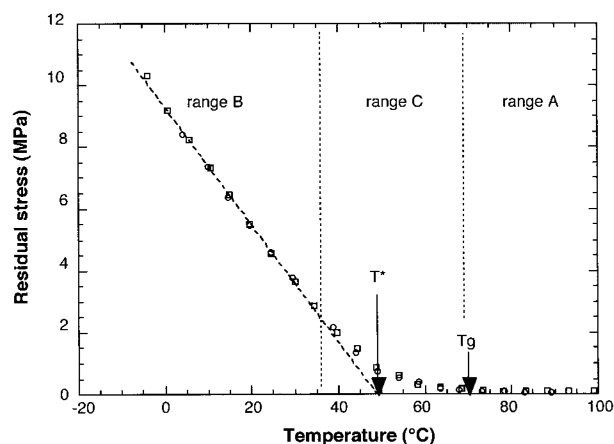

Figure 2 Development of the residual stress, σ_r, as a function of temperature for the network A-1-HA60 (cooling rate: 2 K · min^{-1} ; the circles and squares refer to two independent experiments).

Analysis of Range A

The driving force for producing residual stresses upon cooling ($\alpha_r - \alpha_g$), is enhanced in this temperature range because the networks are above their T_g. Therefore, they exhibit much higher values of α_r than in the glassy state (typically, 2 · 10^{-4} K^{-1} against 6 · 10^{-5} K^{-1}, in order of magnitude) whereas α_g keeps a constant value of about 8 · 10^{-6} K^{-1} all over the temperature range considered. On the other hand, the capacity of the networks to relax the induced stresses is maximum in this range, owing to the high mobility (and low modulus) of the polymer. As illustrated in Figure 2, the balance between the two effects is such that no residual stress is detected over the temperature range T_g + 20°C/T_g. By the way, this observation supports the assumption made in the calculations about the absence of residual stresses at T_g + 20°C. If this assuption was false, it is likely, indeed, that σ_r should vary as cooling the samples down to T_g.

Table III Data for the Analysis of the Residual Stress Values

Network	Stress Development Rate (in Range B) SDR (MPa · K^{-1})	Deformation Development Rate (in Range B) $10^6 \times$ DDR (K^{-1})	Characteristic Temperature of the Range C T^* (°C)	$T_g - T^*$ (°C)	C_1^g	C_2^g (°C)	Apparent Activation Energy at T_g ΔE_a (kJ · mol^{-1})
A-1-DDM	0.140	75	152	36	10.9	35	1265
A-1-BAN60	0.185	67	91	24	9.8	36	865
A-1-BAN80	0.194	69	69	32			785
A-1-BAN95	0.210	71	69	17			740
A-1-DMDDM60	0.196	82	75	38			855
A-0.7-DDM	0.191	55	78	18			780
A-0.8-DDM	0.165	63	105	39			1000
A-0.9-DDM	0.155	75	138	44			1190
A-1.1-DDM	0.147	73	143	34			1165
A-1.2-DDM	0.148	74	134	30			1100
A-1.3-DDM	0.153	78	123	30			1045
A-1-DDM/AP	0.192	68	73	34			830
A-1-DDM/PES-H	0.134		145	38			1195
A-1-DDM/PES-B	0.136		160	28			1220
A-1-HMDA	0.147	89	93	28	11.0	42	780
A-1-HA60	0.191	76	49	21	9.9	34	665
A-1-DMHMDA60	0.213	80	38	22			635
O-1-DDM	0.171	57	93	51			1000
O-1-BAN60	0.203	64	63	22			735
O-1-DMDDM60	0.218	70	58	23			720
O-1-HMDA	0.204	72	56	28			730
O-1-HA60	0.222	65	33	11			580
O-1-DMHMDA60	0.225	65	15	15			530
U-1-DDM	0.186	75	50	28	9.6	27	840
U-1-BAN60	0.231	76	12	20			535

Analysis of Range B

Stress Development Rate, SDR

In the low-temperature range B, the main feature is the linear increase in σ_r, which is observed upon cooling. This behavior can be quantitatively accounted for by considering the slope of the straight line giving the variations of σ_r as a function of temperature. Let us call stress development rate, SDR, the absolute value of this negative slope, expressed in MPa · K^{-1}. The SDRs relative to the different samples under study are given in the first entry of Table III. They vary from 0.134 to 0.231 MPa · K^{-1}, depending on the network under study. Such variations are understandable from eq. (1), which shows that SDR is a function of both Young's modulus and linear thermal expansion coefficient of the resin which are, in turn, functions of the architecture of the network.

From a qualitative viewpoint, this finding can be illustrated by comparing the SDRs of systems presenting the same α_r but different moduli $E_r(T)$ in the glassy state, or vice versa. Arbitrarily, the unknown values of $E_r(T)$ were supposed to be equal to those of storage modulus at 1 Hz, which have been determined by viscoelastic measurements at the same temperatures and very low strain. Thus, the networks A-1-DDM and U-1-DDM exhibit the same α_r but differ by $E_r(T - T_g)$ profiles (Fig. 3): as expected, A-1-DDM, which presents the lower moduli, presents also the lower SDR (Table III). On the contrary, A-1-DDM and A-1-HMDA exhibit roughly identical $E_r(T - T_g)$ profiles (Fig. 4), but very different α_rs, as mentioned above: therefore, A-1-DDM, which presents the lower thermal expansion, also presents the lower SDR.

Quantitatively, the consistency of our measurements can be checked simply, provided some crude assumptions are made. Let us return to the experimental curves of σ_r vs. temperature (example, Fig. 2) and divide, at each temperature, the value of σ_r by that of the elastic modulus, $E_r(T)$, at

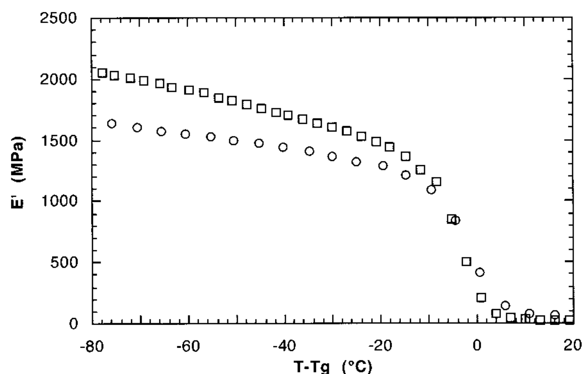

Figure 3 Storage modulus $E'(T, 1\text{ Hz})$ vs. $T - T_g$ for A-1-DDM (open circles) and U-1-DDM (open squares).

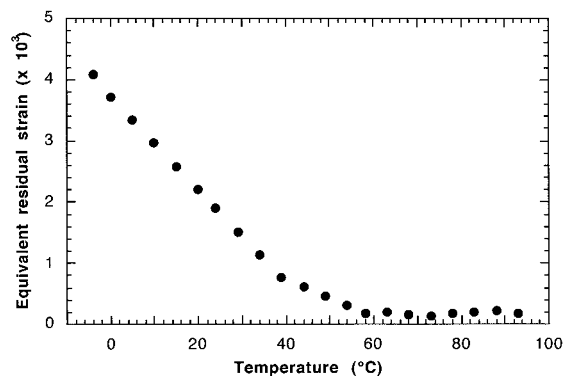

Figure 5 Development of the equivalent residual deformation, $\epsilon_r(T)$, as a function of temperature for the network A-1-HA60).

the same temperature. Again, $E_r(T)$ was replaced, as a first approximation, by $E'(1\text{ Hz}, T)$. As shown in Figure 5 (which has been drawn, as an example, from the experimental data of Fig. 2), the dependence of $\epsilon_r(T)$, defined as

$$\varepsilon_r(T) = \sigma_r(T)/E'(1\text{ Hz}, T) \quad (3)$$

as a function of cooling temperature is given by a straight line. Equation (1) can be rearranged accordingly, by noticing that a and b have the same order of magnitude (2 mm) and that E_r is always small compared to E_g (which equals approximately 75 GPa). It turns out that

$$DDR = \sigma_r/E_r\Delta T \cong \alpha_r - \alpha_g \quad (4)$$

where DDR is called deformation development rate (by analogy to SDR), and has the dimensions of a reciprocal temperature.

As shown in Figure 6, a satisfactory agreement is found between our set of experimental data and eq. (4). The DDRs actually scale as $(\alpha_r - \alpha_g)$, and exhibit similar orders of magnitude. The averaged slope of the plot differs slightly from unity, probably as the consequence of the approximations made, and especially of those on the values of E_r, which have been arbitrarily identified with the available values of $E'(1\text{ Hz})$.

Relationships Between SDR and Network Architecture

In the epoxy networks, the glass transition temperature T_g has been shown to account reliably for the changes in network architecture, whatever changes in chain flexibility, crosslink density, or amount of dangling moities are concerned.[7] Therefore, it is interesting to point out that a global connection holds between SDR and T_g, as shown in Figure 7.

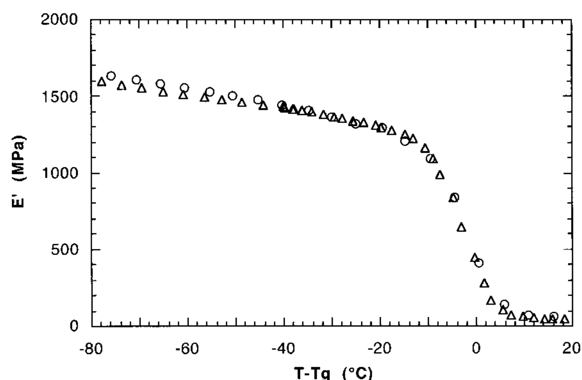

Figure 4 Storage modulus $E'(T, 1\text{ Hz})$ vs. $T - T_g$ for A-1-DDM (open circles) and A-1-HMDA (open triangles).

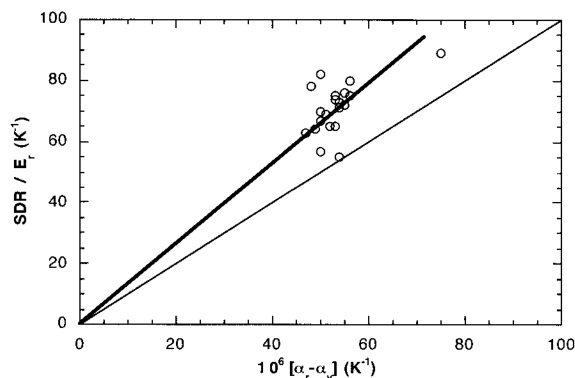

Figure 6 Confrontation of the experimental values of deformation development rate, DDR (K^{-1}), (thick line) to the prediction of eq. (4) (thin line).

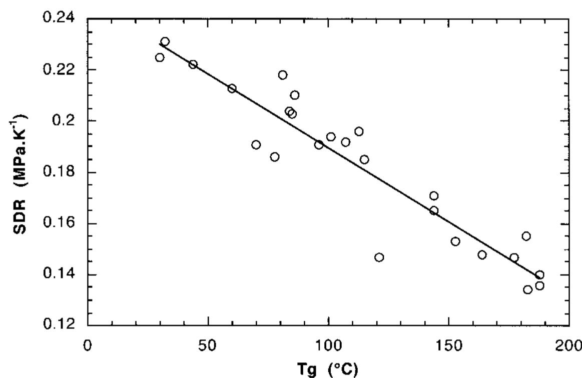

Figure 7 Rate of residual stress development, SDR, as a function of the glass transition temperature, T_g, of the networks.

More detailed analysis of the influence of architecture on the values of SDR needs to put emphasis on the factors that affect the modulus in the glassy state.

It has been pointed out that reduction of crosslink density in networks of identical chain flexibility leeds to a dramatic reduction of the damping associated with the β-relaxation processes as the result of the disappearence of short-scale cooperative motions, and, in turn, to a substantial increase in modulus around room temperature.[7,11,12,25] This result is illustrated in Figure 8, on the example of the series A-1-BAN, but all the series under study behave in the same way. As a consequence of the increase in modulus associated with the decrease of crosslink density, SDR is also increased (Table III). This general feature is shown in Figure 9(a) and (b), in the case of the different diepoxides in the presence of the two types of chain extensors.

In dense networks (prepared in the absence of a cohardener), departure from the stoichiometric ratio $r = 1$ leads to reduction of both crosslink density[7] and β-relaxation damping [Fig. 10(a)] and to a marked increase in modulus in the glassy state [Fig. 10(b)]. As expected, progressive increase of SDR is associated with the decrease of crosslink density (Fig. 11). The effect of the undercure of stoichiometric mixtures (not shown here) would be the same: because the limitation of the extent of epoxide/amine reaction leads to a fortified modulus at room temperature, it also gives rise to an enhancement of SDR.

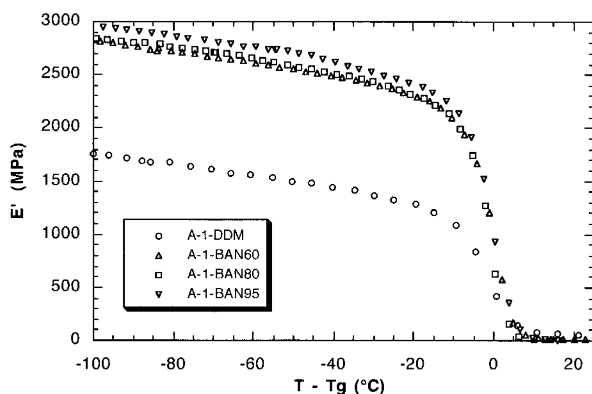

Figure 8 Storage modulus $E'(T, 1\text{ Hz})$ vs. $T - T_g$ for the A-1-BAN series.

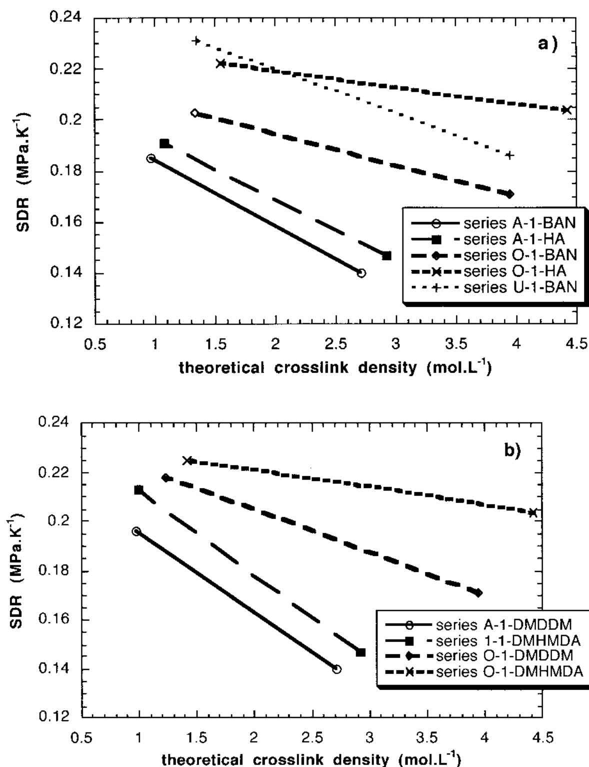

Figure 9 Dependence of the SDRs on the reduction in crosslink density resulting from the use of cohardeners: (a) primary monoamines; (b) secondary diamines.

Analysis of Range C

Range C extends from a temperature close to T_g down to the temperature at which σ_r comes to increase linearly with decreasing temperature. Because the actual limits of range C are not easy to quantify with confidence from the experimental data, it was conventionally accounted for its extent by considering the gap between T_g and T^*, where T^* represents the interpect with the T-axis of the straight line defining the variations of σ_t vs. T in range B (see Fig. 2).

As shown in the forth entry of Table III, the quantity $(T_g - T^*)$ varies markedly from one net-

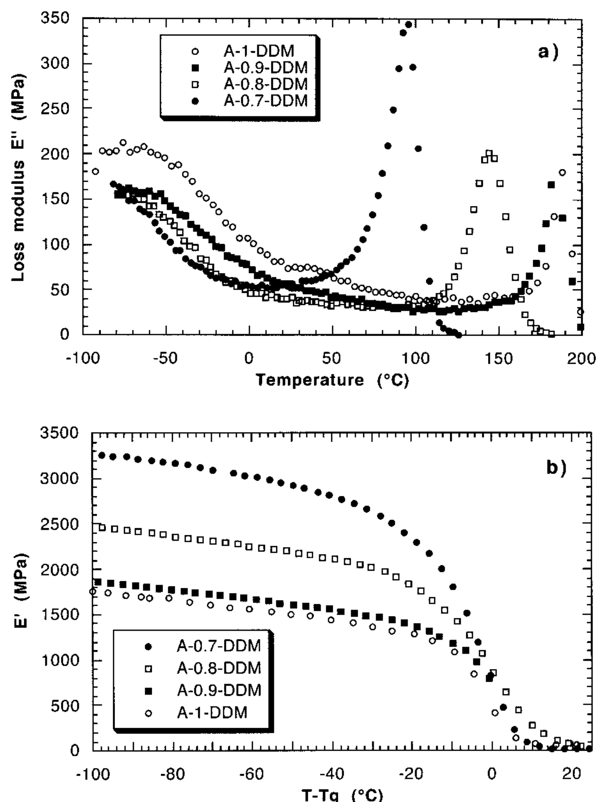

Figure 10 Viscoelastic traces at the frequency 1 Hz relative to the networks A-DDM prepared with various stoichiometric ratios r ($0.7 \leq r \leq 1$): (a) Loss modulus $E''(T, 1\text{Hz})$ vs. temperature; (b) storage modulus $E'(T, 1\ \text{Hz})$ vs. $T - T_g$.

work to the other, in the range of 11–51°C. Range C represents the temperature range where the networks remain able, with a delayed response, to relax the stresses resulting from the difference in

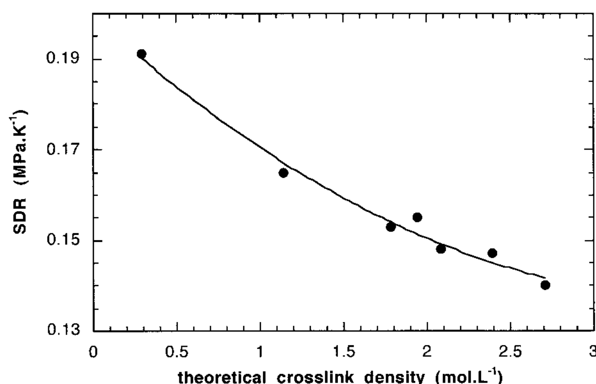

Figure 11 Rate of residual stress development, SDR, as a function of the crosslink density of A-DDM networks prepared with various stoichiometric ratios r ($0.7 \leq r \leq 1.3$).

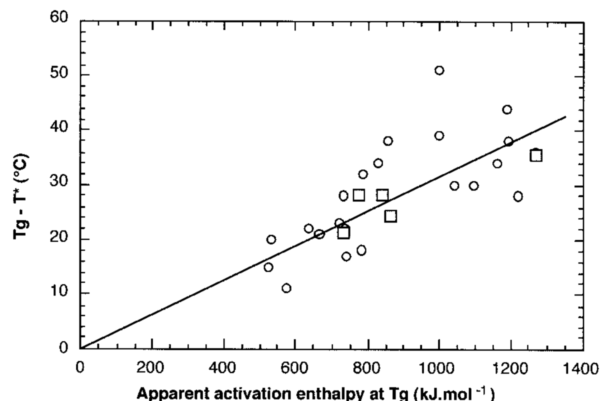

Figure 12 Extent of the range C of residual stress development as a function of the apparent activation energy at T_g.

thermal expansion of glass and resin. As a consequence ($T_g - T^*$) is influenced by the viscoelastic characteristics of the network in the glass transition region. For this reason, we propose to link up ($T_g - T^*$) to the apparent activation energy of the glass transition temperature, $\Delta E_a(\mathrm{T})$. According to the Williams-Landel-Ferry (WLF) approach of the glass transition phenomena,[29] $\Delta E_a(T)$ and $\Delta E_a(T_g)$, relative to the temperatures T and T_g, respectively, are given by the equations

$$\Delta E_a(T) = 2.303R\,\frac{C_1^g C_2^g T^2}{(C_2^g + T - T_g)^2} \tag{5}$$

$$\Delta E_a(T_g) = 2.303R\,\frac{C_1^g T_g^2}{C_2^g} \tag{6}$$

where T_g is given in Kelvin, R is the gas constant and $C^g{}_1$ and $C^g{}_2$ are the WLF viscoelastic coefficients taken at T_g as the reference temperature. For some networks, namely A-1-DDM, A-1-HMDA, A-1-BAN60, A-1-HA60, and U-1-DDM (Table III), the values of the viscoelastic coefficients are available in the literature,[7] so that $\Delta E_a(T_g)$ can be calculated with confidence from eq. (6). In this case, a very good correlation is found between $\Delta E_a(T_g)$ and ($T_g - T^*$), as shown by the open squares in Figure 12. For the others, $\Delta E_a(T_g)$ was estimated by making the very crude assumption that the ratio of $C^g{}_2$ to $C^g{}_1$ would take the value 0.3 (which is the average value relative to the known systems), irrespective of the network considered. Despite the scattering of the data shown in Figure 12, owing in part to the lack of precision on activation energy values, it is

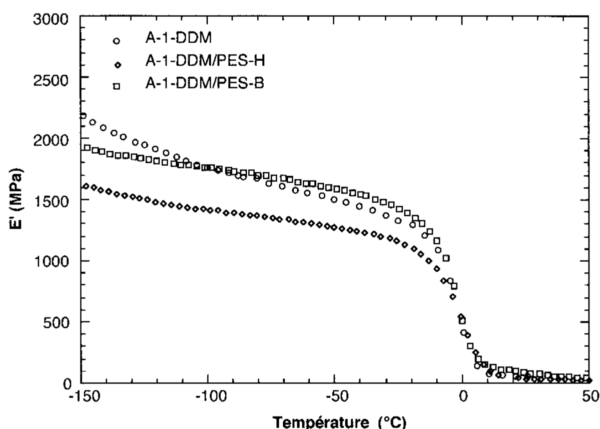

Figure 13 Storage modulus $E'(T, 1\ \mathrm{Hz})$ vs. temperature for the homogeneous and biphasic networks A-1-DDM/PES (the trace relative to pure A-1-DDM is also recalled, for the sake of comparison).

worth noting that the scaling of $(T_g - T^*)$ as the square of T_g seems to be suitable.

Residual Stresses in Epoxy Networks of More Complex Formulation

The antiplasticized network A-1-DDM/AP presents the same thermal expansion as the pure system A-1-DDM (Table II). On the other hand, it exhibits a much higher modulus at room temperature than its pure counterpart, in agreement with the molecular mechanism of antiplasticization detailed elsewhere.[13,14,25] As expected from the analyses given in the previous sections, A-1-DDM/AP actually presents a markedly higher value of SDR than A-1-DDM (Table III). A supplementary check on the behavior of this system can be made by noticing that it presents roughly the same characteristics of interest here (T_g, α_r, modulus around room temperature) as the network A-1-80BAN. As shown in Table III, a remarkable similarity is observed on all the residual stress descriptors (SDR, DDR, $T_g - T^*$) of the two networks.

The thermal expansion coefficient is the same for the two networks filled with polyethersulfone, whatever they are homogeneous (A-1-DDM/PES-H) or biphasic (A-1-DDM/PES-B), and it is slightly lower than that found for the pure network A-1-DDM (Table II). As shown in Figure 13, the glassy state moduli (in the temperature range to be considered for a comparison of the SDRs) rank in the order: $E_{\text{A-1-DDM/PES-H}} < E_{\text{A-1-DDM}} \cong E_{\text{A-1-DDM/PES-H}}$. Because A-1-DDM/PES-H presents a lower modulus and a higher thermal expansion than A-1-DDM, there are two reasons so that it presents a lower SDR, as can be seen in Table III. One may argue from lower thermal expansion and roughly identical modulus to try to explain why A-1-DDM/PES-B has a lower SDR than A-1-DDM. On the other hand, the fact that A-1-DDM/PES-H and A-1-DDM/PES-B are characterized by quasi-identical SDRs cannot be understood on these bases. However, it is worth noticing, as an important point for the applications, that the addition of a thermoplastic polymer in the epoxy resin formulations has a supplementary benefit in addition to those already mentioned in the literature:[30–32] the addition of polyethersulfone is shown in the present study to provoke a reduction of the sensitivity of the epoxies to the formation of residual stresses.

CONCLUSIONS

From this study of various epoxy-amine networks, it turns out that the thermal expansion coefficient is only slightly affected (with a few noticeable exceptions) by the architectural characteristics. On the other hand, modulus in the glassy state is strongly influenced by the crosslink density, in a way that can be rationalized on the basis of a detailed analysis of the secondary relaxation motions. As a consequence, any change in crosslink density has repercussions on the modulus of the network and, in turn, on its ability to develop residual stresses. Besides, the results are at the opposite of what would be guessed intuitively: the lower the crosslink density, the higher the stress development rate upon cooling.

However, in the view of the applications, one should beware of this finding, because the reduction of crosslink density is also accompanied by a decrease of T_g. Depending on which of the two competing effects prevails, the effect of crosslink density on the overall stress accumulated at room temperature can be reversed. Let us compare, as a typical example, the networks A-1-DDM and A-0.7-DDM, whose crosslink density is a tenth that of the former, and whose SDR is 0.191 MPa $\cdot\ \mathrm{K}^{-1}$ against 0.14 MPa $\cdot\ \mathrm{K}^{-1}$. Just because the T_g of A-0.7-DDM (78°C) is much lower than that of A-1-DDM, then the overall stress accumulated when cooling from T_g down to room temperature will be only 10 MPa in the loosely crosslinked network, instead of 18 MPa in the dense network.

This work was supported by the French Ministry of Defence (DGA/DRET) under contract No. 92 1218.B/DRET. The authors are grateful to Dr. G. Gallicher

(DRET) and Drs. J. P. Favre and B. Bloch (ONERA, Châtillon, France) for their interest to this study. They also wish to thank Prof. J. Verdu (ENSAM, Paris, France) for kind and stimulating discussions on the thermal expansion of epoxies.

REFERENCES

1. Dusek, K., Ed. Adv Polym Sci 1985, 72, 1.
2. Dusek, K., Ed. Adv Polym Sci 1986, 75, 1.
3. Dusek, K., Ed. Adv Polym Sci 1986, 78, 1.
4. Halary, J. L.; Cukierman, S.; Monnerie, L. Bull Soc Chim Belg 1989, 98, 623.
5. Cukierman, S.; Halary, J. L.; Monnerie, L. J Non-Cryst Solids 1991, 131–133, 898.
6. Gallouedec, F.; Costa-Torro, F.; Lauprêtre, F.; Jasse, B. J Appl Polym Sci 1993, 47, 823.
7. Halary, J. L.; Bauchière, D.; Lee, P. L.; Monnerie, L. Polimery 1997, 42, 86.
8. Gérard, J. F.; Galy, J.; Pascault, J. P.; Cukierman, S.; Halary, J. L. Polym Eng Sci 1991, 31, 615.
9. Won, Y. G.; Galy, J.; Gérard, J. F.; Pascault, J. P.; Bellenger, V.; Verdu, J. Polymer 1990, 31, 1787.
10. Yang, L.; Hristov, H. A.; Yee, A. F.; Gidley, D. W.; Bauchière, D.; Halary, J. L.; Monnerie, L. Polymer 1995, 36, 3997.
11. Cukierman, S.; Halary, J. L.; Monnerie, L. Polym Eng Sci 1991, 31, 1476.
12. Heux, L.; Halary, J. L.; Lauprêtre, F.; Monnerie, L. Polymer 1997, 38, 1767.
13. Heux, L.; Lauprêtre, F.; Halary, J. L.; Monnerie, L. Polymer 1998, 39, 1269.
14. Merritt, M. E.; Goetz, J. M.; Whitney, D.; Chang, C. P. P.; Heux, L.; Halary, J. L.; Schaefer, J. Macromolecules 1998, 31, 1214.
15. Aboulfaraj, M. Thesis, University Louis Pasteur (Strasbourg 1) (1989).
16. Wippler, C.; Aboulfaraj, M.; Schirrer, R.; Pixa, R. Polym Compos 1988, 9, 125.
17. Halary, J. L.; Bauchière, D.; Monnerie, L.; Schirrer, R. 4th Meeting of the MTS Elastomer Testing Users Society, Paris, France, September 1995.
18. Bloch, B. ONERA Châtillon (France), personal communication.
19. Dobas, I.; Eicheir, J. Czech Chem Commun 1973, 38, 2602.
20. Daly, A.; Britten, A.; Garton, A.; McLean, P. D. J Appl Polym Sci 1984, 29, 1403.
21. Halary, J. L.; Oultache, A. K.; Louyot, J. F.; Jasse, B.; Sarraf, T.; Muller, R. J Polym Sci Polym Phys Ed 1991, 29, 933.
22. Tordjeman, P.; Tézé, L.; Halary, J. L.; Monnerie, L. Polym Eng Sci 1997, 37, 1621.
23. Brandup, J.; Immergut, E. H.; Polymer Handbook; Wiley-Interscience: New-York, 1989.
24. Cukierman, S. Thesis of the University PM Curie Paris (1991).
25. Halary, J. L.; Heux, L.; Rana, D.; Sauvant, V.; Monnerie, L. Proc Am Chem Soc Div Polym Mat Sci Eng 1996, 75, 358.
26. Lee, B.; Hartmann, B. J Appl Polym Sci 1984, 28, 823.
27. Bellenger, V.; Dhaoui, W.; Morel, E.; Verdu, J. J Appl Polym Sci 1988, 35, 563.
28. Merritt, M. E.; Heux, L.; Halary, J. L.; Schaefer, J. Macromolecules 1997, 30, 6760.
29. Ferry, J. D. Viscoelastic Properties of Polymers; Wiley: New York, 1980, 3rd ed.
30. Yamanaka, K.; Inoue, T. Polymer 1989, 30, 622.
31. Akay, M.; Cracknell, J. G. J Appl Polym Sci 1994, 52, 663.
32. Horiuchi, S.; Street, A. C.; Ougizawa, T.; Kitano, T. Polymer 1994, 35, 5283.